Real-Time Imaging of *Mycobacterium tuberculosis* Using a Novel Near-Infrared Fluorescent Substrate

Hee-Jeong Yang[1,a], Ying Kong[2,a], Yunfeng Cheng[3,a], Harish Janagama[1], Hany Hassounah[1], Hexin Xie[3], Jianghong Rao[3], and Jeffrey D. Cirillo[1,b]

[1]Department of Microbial Pathogenesis and Immunology, Texas A&M Health Science Center, Bryan, TX 77807

[2]Department of Microbiology, Immunology and Biochemistry, University of Tennessee Health Science Center, Memphis, TN 38163

[3]Department of Radiology, Stanford University, Stanford, CA 94305

[b]Corresponding author: JDCirillo@medicine.tamhsc.edu Tel. 979-436-0343

[a]These authors contributed equally to this work.

Abstract

Slow growth of *Mycobacterium tuberculosis* (Mtb), the causative agent of tuberculosis (TB), hinders advancement in all areas of research toward prevention and treatment. Real time imaging, employing reporter enzyme fluorescence (REF) that uses custom fluorogenic substrates for bacterial enzymes, allows rapid and specific detection of Mtb in live animals. We have synthesized a novel REF substrate, CNIR800, which carries a near-infrared (NIR) fluorochrome IRDye 800CW, with a quencher connected through the lactam ring that is hydrolyzed by the enzyme BlaC (β-lactamase) naturally expressed by Mtb. CNIR800 produces long wavelength emission at 795 nm upon excitation (745 nm) and exhibits significantly improved signal-to-noise ratios for detection of Mtb. The detection threshold with CNIR800 is ~100 colony forming units (CFU) *in vitro* and <1000 CFU in the lungs of mice. Additionally, fluorescence signal from cleaved CNIR800 reaches maximal levels at 4-6 h post-administration in live animals, allowing accurate evaluation of anti-tuberculous drug efficacy. Thus, CNIR800 represents an excellent substrate for accurate detection of Mtb rapidly and specifically in animals, facilitating research toward understanding pathogenic mechanisms, evaluation of therapeutic outcomes, and screening new vaccines.

Tuberculosis (TB), caused by *Mycobacterium tuberculosis* (Mtb), is one of the most frequent causes of mortality in humans due to a single infectious agent. One-third of world's population is infected with TB [1] and ~9 million people become newly infected each year, leading to 1.5 million TB-related deaths (CDC 2013). Mtb spreads via aerosol droplets from one infected individual to another and initially infects the lungs. Early diagnosis is key to identifying of new cases and treating them efficiently to help reduce additional TB infections and TB related deaths. However, the absence of effective vaccines and slow growth rate of Mtb impede efficient diagnosis in the early stages of TB infection.

The great potential of optical imaging technologies to profoundly impact TB research has recently been recognized [2]. Fluorescent proteins (FP), bioluminescence, and reporter enzyme fluorescence (REF) have been employed for optical imaging and successfully used for detection of Mtb in live animals in real time [2-7]. The major advantages of optical imaging are rapid and specific assessment of Mtb infection compared to conventional colony-forming units (CFU)-based method, which requires 4-6 weeks to complete assessment [2-6, 8].

Reporter enzyme fluorescence (REF), which uses the enzyme BlaC (β-lactamase), naturally constitutively expressed by *Mycobacterium* [9, 10] and custom fluorogenic substrates [2, 4], has shown great promise for the use in optical imaging to detect Mtb because of its specificity and sensitivity [2, 4]. Near-infrared (NIR) fluorophores are preferred for *in vivo* imaging because longer emission wavelengths within the near-

infrared region overcome most sources of photon attenuation in living animals (Li-Cor, [11]). In the REF system, fluorophores are customized by linking them to a quencher at the distal end through a lactam ring, which can be hydrolyzed by BlaC. In the absence of BlaC, the fluorochrome is quenched and does not fluoresce greatly; but in the presence of BlaC, substrate becomes fluorescent by cleavage of the lactam ring and loss of the quencher. In this manner, REF catalytic activity generated directly from the bacteria allows amplification of signal and sensitive detection of Mtb, without genetic modification. This prevents unwanted effects on virulence and enables immediate use with any Mtb strain, including those present in infected patients or clinical samples.

BlaC-specific REF substrates can be used for both pre-clinical and clinical TB research. Substrates CDG-OMe and CDG-3 are based on a modified cephalosporin and have been used to detect Mtb in sputum samples with good sensitivity and specificity [12, 13]. CNIR5, which carries the fluorophore Cy5.5, has been used for non-invasive imaging in live animals infected with Mtb, resulting in a detection limit of ~10^4 CFU in the lungs [2]. An improved detection threshold is desirable due to the low infectious dose of TB (1-10 CFU). Additionally, tissue penetration of excitation and emission light in live animals is likely a key limitation that must be overcome to improve the threshold of detection for REF beyond that of CNIR5. We hypothesized that the sensitivity of REF imaging could be improved by replacing Cy5.5 with IRDye 800CW, which has a longer excitation and emission wavelength. Our expectation from a longer wavelength substrate was improved tissue penetration and reduced background [11].

We developed an improved longer wavelength REF imaging substrate, CNIR800, that displays significantly increased signal-to-noise ratios for detection of Mtb with a threshold of ~100 CFU *in vitro* and <1000 CFU in the lungs of mice *in vivo*. Maximal signal-to-noise ratios were achieved at ~6 h post-administration of CNIR800 and the fluorescent signal correlated well with CFU in the lung (R^2=0.87, P<0.0001). Furthermore, CNIR800 could also be utilized for rapid evaluation of therapeutic efficacy, confirming that REF imaging can be used to facilitate research toward novel TB interventions.

METHODS

Strains and Growth Conditions

Mycobacterium tuberculosis (Mtb) strain CDC1551, Erdman, bacillus Calmette-Guérin (Pasteur, BCG) and derivatives were used for all experiments. All strains were grown as described previously [14]. Additional details are included in Supplementary Methods.

Design and synthesis of CNIR800

CNIR800 was designed and synthesized as described previously with some modifications [2]. Details are included in Supplementary Methods.

Animal Infections

All animal experiments in this study were approved by Texas A&M University Institutional Animal Care and Use Committee. Five- to seven-week old female BALB/C

mice were fed commercial alfalfa-free diet (Harlan Teklad, Indianapolis, IN) with *ad libitum* access to tap water. Mice were infected with a broad range (~10^3-10^7 CFU) of bacteria by several different routes as described previously [5, 6, 15]. Bacterial numbers were determined by plating 10-fold dilutions of the homogenized tissue on the 7H11 selective media. Therapeutic studies used 3 different concentrations of isoniazid (INH) at 5 mg, 1 mg, and 0.1 mg/kg, given to mice daily by intraperitoneal injection beginning at 2 weeks post-infection for 4 weeks. At least 4 mice per group were infected for each experimental group, unless stated otherwise. Additional details are included in Supplementary Methods.

Imaging Mycobacterial Infections

Imaging was performed as described previously [5, 6]. Details are included in Supplementary Methods.

Statistical Analyses

Statistical significance was determined using a Student's two tailed t-test or ANOVA with significance set at $P < 0.05$. To determine the relationship between CFU and fluorescence, linear regression analyses and Pearson's correlation were used.

RESULTS

Design and Characterization of CNIR800

The fluorogenic probe CNIR800 was constructed by linking a near-infrared fluorescence dye, IRDye 800CW, to a quencher, IRDye QC-1, through the lactam ring, allowing fluorescence resonance energy transfer (FRET)-based quenching (Figure 1*A*). The probe was purified by HPLC and the structure was confirmed by MALDI-MS (Supplementary Figure 1, $C_{142}H_{174}ClN_{14}O_{46}S_{12}^{+}$ m/z 3230.903 $M+H^{+}$). IRDye 800CW is an excellent candidate for use in *in vivo* imaging due to improved tissue penetration, reduced light scattering, and decreased auto-fluorescence [11]. Upon the cleavage of the lactam ring by the Mtb BlaC*,* CNIR800 releases the quencher IRDye QC-1 and the molecule becomes fluorescent (Figure 1*B* and 1*C*). Cleaved CNIR800 displays maximal signal at an excitation wavelength of 745 nm and emission of 795 nm (Figure 1*B*). This substrate exhibits ~20-fold increase in fluorescence after 10 minutes incubation with BlaC and fluorescent signal remains near maximal for at least 120 minutes after cleavage (Figure 1*C*).

Detection of *Mycobacterium* Using CNIR800 *in vitro*

We first detected *Mycobacterium* using substrate CNIR800 in J774A.1 murine macrophage cells infected with a GFP expressing *M. bovis* BCG strain and co-incubated with CNIR800 for 30 minutes. M. *bovis* BCG strains have been used to facilitate standardization of conditions for imaging at Biosafety Level 2 (BSL2). BCG is not virulent for humans, but retains similar infection and persistence as pathogenic mycobacteria

within mammalian tissue [16]. As shown in Figure 2*A*, fluorescent signal that arises from CNIR800 is found in small vesicles throughout the cytoplasm of infected macrophages and, in some cases, is co-localized with the bacterial vacuole. These observations demonstrate that CNIR800 is a cell permeable substrate and the fluorescent product incorporates into infected cells, rather than being lost after cleavage. This observation is consistent with the data obtained with the previous generation REF substrate, CNIR5 [2]. We also observed that fluorescent signal correlates well with CFU over a broad range of bacterial numbers from 10 to 10^5 CFU (R^2=0.92) (Figure 2*B*). However, the signal obtained from 100 CFU and above was significantly greater than the background (10^0 group, P=0.04). Thus, CNIR800 can be used for quantitative detection of Mtb infection intracellularly.

Kinetics of CNIR800 Tissue Distribution in Mice

We performed pharmacokinetic and tissue distribution analyses of CNIR800 in naïve (uninfected) animals. Blood and organs were collected from naïve animals at different time points after intraperitoneal (I.P) administration of CNIR800. We evaluated fluorescence generated by intact and cleaved substrate in the absence and presence of BlaC in these blood (Figure 2*C* and 2*D*) and organ samples (Figure 3). Levels of intact CNIR800 in the blood of naïve mice peaked at 3 h post-administration and fluorescent signal was greatly reduced by 24 h (Figure 2*C* and 2*D*). Fluorescent signal was significantly higher in the BlaC treatment group at most of time points compared to the no treatment group. At 24 h, we observed that despite reduction of total amount of

substrate in the animal system, most of it is intact giving a significantly higher signal when cleaved with BlaC (Figure 2*D*). Fluorescent signal was not detectable after 24 h post-administration (data not shown). We also observed basal levels of background fluorescent signal in the blood without BlaC treatment, most likely due either to high levels of quenched substrate or low levels of spontaneous hydrolysis of substrate. Non-specific hydrolysis of the substrate may occur at low levels due to reaction with serum albumin, which exists in blood and has been known to have lactamase activity on other lactam substrates [17, 18]. Similar results were observed when examining fluorescence levels due to CNIR800 in other organs, with a maximum at 5 h post-administration of the substrate (Figure 3). Tissue distribution of CNIR800 was the highest in kidneys at early time points, consistent with a previous study showing that the kidney serves as a primary clearance and excretion route for IRDye 800CW [19].

We next examined the kinetics of CNIR800 in mice infected with Mtb. Mice were infected via the subcutaneous (Supplementary Figure 2), intravenous (Figure 4), or intratracheal route (Supplementary Figure 3). At 24 h post-infection, CNIR800 was delivered to mice intraperitoneally and fluorescent signal was measured over time. In these studies we evaluate lung signal kinetics because planned experiments were focused on lung infection. Because of this focus, animal whole body imaging used only illumination points around where the lungs were expected to be located. Images were acquired with 9-12 trans-illumination points around the area that was expected to contain the lungs. In this manner, we optimizes the signal kinetics and imaging for experiments where our infection route is intratracheal or aerosol, the focus of most

tuberculosis studies, since aerosol is the natural route of infection. Fluorescence increased in accordance with the number of bacteria present regardless of the infection route (Supplementary Figure 2 and Supplementary Figure 3) and significantly increased from 4 h post-administration, reaching maximal levels at 6 h post-administration (Figure 4, Supplementary Figure 2 and Supplementary Figure 3). In addition to whole body imaging, we measured fluorescence in *ex vivo* lung tissue. We observed similar results to those with *in vivo* imaging, the increase in fluorescence was significant in the lungs from 4 h post-administration, reaching maximal levels at 6 h post-administration (Figure 4*B*). These data confirm that the *in vivo* fluorescence is due to the signal arising from the lungs.

Real-Time Imaging to Detect *Mycobacterium* in Live Animals

To define the parameters and detection threshold of CNIR800, we evaluated fluorescence levels obtained in animals infected with different bacterial CFU in the lungs. Mtb strain CDC1551 was delivered to groups of mice by intratracheal infection and the substrate was administered at 24 h post-infection intraperitoneally. Fluorescence was measured at 6 h post-administration of CNIR800 with an IVIS spectrum using trans-illumination for whole body images and epi-illumination for lung tissues. Following *ex vivo* lung imaging, lung tissue was homogenized and plated to enumerate bacterial numbers. Fluorescence increased in accordance with the bacterial numbers in whole body images (Figure 5*A*) with a limit of detection < 10^3 CFU, similar results were also obtained for *ex vivo* lung tissue (Figure 5*B*). The fluorescence signal correlated well with

bacterial numbers both in whole body images (R^2=0.87, P<0.0001) and *ex vivo* lung images (R^2=0.81, P=0.0001) (Figure 5*C* and 5*D*). This correlation is sufficient to allow accurate quantification of bacterial numbers by real-time imaging using CNIR800 in place of CFU.

We have also investigated Mtb infection in guinea pigs, which are known to be an important model for human TB [20-22] and have increased tissue depth compared to mice. As shown in Supplementary Figure 5, we observed significantly higher fluorescence in infected guinea pigs as compared to uninfected animals (Supplementary Figure 5*A*-5*C*) and fluorescence correlated well with bacterial CFU (Supplementary Figure 5*D*). These observations demonstrate that CNIR800 can be used for tracking Mtb infections in animals that are larger than mice.

We further monitored a physiologically relevant dose of Mtb (<10^2 CFU) during infection in the lungs of live animals by imaging with CNIR800. Fluorescence increased significantly in infected animals from 14 days to 42 days post-infection, suggesting that CNIR800 allows quantitative detection of Mtb during pulmonary infection of live animals (Figure 6). We also investigated whether CNIR800 is capable of tracking a high dose of Mtb (~10^3 CFU) during infection. Mtb was delivered to mice using the Madison chamber and fluorescence was measured with CNIR800. As shown in Supplementary Figure 4, we detected higher fluorescence in infected animals as compared to uninfected animals on days 21 and 60 post-infection, suggesting that CNIR800 is successful in tracking Mtb during high dose pulmonary infection. Interestingly, fluorescence on days 21 and 60 was lower than on day 1 (Supplementary Figure 4) and, similarly, in another experiment at

15 and 24 weeks fluorescence was low, despite CFU remaining relatively steady throughout this period (Figure 6*B* and 6*C*). The mice increased in body weight by an average of 2.8 (P=0.007) and 5.1 grams (P=0.0001) at 15 and 24 weeks as compared to week 1. Since the mice during each of these experiments gained body mass and volume, we believe that these observations are due to either the increase in size of the animals reducing the ability of the excitation wavelength to penetrate to the lungs or granulomas. These observations suggest that REF imaging works well when mice are small or early infection to allow efficient imaging, but drops off in utility as the animals get larger or later infection phase.

Determining Therapeutic Efficacy With CNIR800

We infected mice with Mtb by aerosol and treated animals to cure infection with different concentrations of isoniazid (INH, 5.0, 1.0, and 0.5 mg/kg, I.P) daily, an antibiotic that is part of the first-line of therapies for human tuberculosis, starting at 2 weeks post-infection for 4 weeks. Antimicrobial efficacy was evaluated by REF imaging using CNIR800 and compared to conventional CFU-based methods. As shown in Figure 6, fluorescence was higher in infected animals at 1 week post-infection. At 2 weeks post-infection, prior to initiating INH treatment, similar levels of fluorescence were observed in treated and untreated animals. However, fluorescence decreased in INH treated (5 mg) animals by week 4 and the reduction in fluorescence was more obvious by week 6 at the end of treatment (INH 5 mg) (Figure 6*B*). Fluorescence increased in untreated animals and animals treated with sub-therapeutic concentrations of INH (1 mg or 0.5 mg)

(Figure 6*D*). Similar to fluorescence, bacterial numbers as measured by conventional CFU assays decreased during treatment with 5 mg of INH at 6 weeks, but, as expected, treatment with lower concentrations exhibited increased CFU (Figure 6*C* and 6*E*). Recovery of CFU post-treatment was observed due to re-growth of bacteria after partial sterilization, since treatment terminated at 6 weeks (Figure 6*C*). These observations demonstrate that REF imaging with CNIR800 can be used to evaluate therapeutic efficacy more rapidly than conventional CFU-based methods. In contrast, CFU-based assays would require growth of the bacteria, taking approximately 4 additional weeks; whereas, REF imaging provides an immediate result. These observations raise the possibility that similar REF strategies could be applied to rapidly demonstrate therapeutic outcomes in humans clinically.

DISCUSSION

A limitation of optical imaging is depth penetration due to light scattering in tissue [23, 24]. In the NIR spectral region (700-900 nm), the least tissue absorption and light scattering by water, oxyhemoglobin (HbO_2), deoxyhemoglobin (Hb), and fat is observed. Hence, NIR fluorophores are considered nearly optimal for optical imaging. In this study, we developed and characterized a novel NIR substrate for non-invasive optical REF imaging to detect Mtb in live animals. CNIR800 carries IRDye 800CW, a NIR fluorophore linked to a quencher by a lactam ring, which can be hydrolyzed by the Mtb β–lactamase, BlaC. Upon cleavage of the substrate by the naturally constitutively expressed BlaC, CNIR800 becomes fluorescent, resulting in the ability to detect Mtb quantitatively in

nearly any mammalian tissue or clinical material. Our new substrate CNIR800 displays numerous advantages. The fluorophore, IRDye 800CW used for CNIR800 has been rigorously evaluated for toxicity, demonstrating no harmful effects in mammals [19]. Clearance half-life of IRDye 800CW has been reported to be 35.7 min. and 236.5 min. following IV and ID injection respectively [19]. Additionally, our pharmacokinetic studies with CNIR800 demonstrate that most of fluorescent product in the blood and organs is cleared by 24 h after administration of the substrate (Figure 3). Furthermore, this dye has been used for molecular imaging in clinical studies with cancer and infectious disease [25-28]. Thus, this novel NIR substrate, CNIR800 would accelerate use for translational tuberculosis imaging in humans.

We employed REF imaging with BlaC, a strategy for non-invasive optical imaging for tracking TB infection in live animals in real-time [2, 4]. REF imaging using BlaC displays great promise for *in vivo* optical imaging in small animals and possibly larger mammals as compared to alternative approaches using fluorescent proteins (FP) or bioluminescence [2-6, 8] due to its great sensitivity and specificity [2]. BlaC represents an excellent bio-marker for Mtb because it is conserved in the Mtb-complex, including BCG and all Mtb clinical isolates [29] but is not produced by mammals. There are some other organisms that produce β-lactamase, but REF substrates have been produced that are highly specific to Mtb BlaC [30]. We also have examined many *M. tuberculosis* genome databases (http://www.sanger.ac.uk/resources/downloads/bacteria/mycobacterium.html, http://genome.tbdb.org/tbdb_sysbio/MultiHome.html), showing that there are no

naturally existing Mtb mutants in *blaC* that would result in loss of the functional beta-lactamase. The enzyme BlaC is surface localized and constitutively expressed, eliminating the need for the fluorogenic substrate to gain access to the bacterial cytoplasm [2, 9, 29, 31, 32]. Furthermore, BlaC is secreted via the twin-arginine translocation (TAT) pathway, enabling analysis of Mtb viability based on levels of BlaC activity [33-35]. Lastly, since REF measures enzyme catalytic activity through cleavage of the substrate by endogenously expressed BlaC, it is not limited solely by the number of protein molecules produced. The cleaved fluorescent product appears to be retained in the host cell and fluorescent signal continues to build up as long as substrate is available. This allows greater sensitivity than fluorescent proteins (FP) or bioluminescence, which are limited by levels of protein that can be produced in bacteria or the levels of substrate that can gain access to Mtb during the imaging period, respectively. However, in our *in vivo* pharmacokinetic study, we observed the substrate CNIR800 was cleared by 24 h in the blood and organs of mice after administration of a single bolus of substrate. It is likely that additional administration of substrate prior to complete clearance of the cleaved product that results in signal would allow product to build up in the host cell, increasing fluorescent signal overall, resulting in improved sensitivity. Additionally, REF can be used to detect Mtb-complex without any genetic modification, enabling potential use for quantitative detection of Mtb directly in all infection models, clinical materials and patients.

Previously, Ying et al. have developed the REF substrate, CNIR5, which carries Cy5.5 (Abs Max at 678 nm, Em Max at 701 nm), and successfully imaged Mtb infection in

mice [2]. CNIR5 displayed maximal signal between 24-48 hours post-administration and allowed detection of Mtb infection with a threshold of 10^4 CFU in mouse lungs. The longer wavelength of IRDye 800CW (Abs Max at 774 nm, Em Max at 789 nm) allows improved tissue penetration and reduced light scattering in mammalian tissue, reducing auto-fluorescence. We observed that CNIR800 can detect ~100 CFU of Mtb in excised lung tissue and <1000 CFU in the lungs of live animals (Figure 2*B* and Figure 5). This demonstrates that CNIR800 is ~10-fold more sensitive than CNIR5 [2]. Pharmacokinetics of CNIR800 are faster than those of CNIR5, displaying maximal signal between 5-7 hours post-administration. The more rapid distribution of CNIR800 would be beneficial for clinical applications, since patients would not need to remain in the clinic for extended periods prior to imaging.

Our *in vitro* observation of intracellular mycobacteria using CNIR800 (Figure 2*A* and 2*B*) demonstrates that CNIR800 can be used for *in vitro* cellular quantification of mycobacteria, replacing conventional CFU assays. In addition, substrate pharmacokinetic studies (Figure 2*C,* 2*D* and Figure 3) provide useful and valuable information for further clinical use of CNIR800. For clinical administration of the REF substrate, intravenous delivery would work well [2], but it is also likely that aerosol delivery, particularly for lung imaging, would display good tissue distribution. Application of CNIR800 to late phases of infection will require further modification and optimization to improve sensitivity. In our pilot experiments using guinea pigs, CNIR800 allows detection of Mtb in deep tissue (Supplementary Figure 5). This observation is very exciting and is promising for the development of new clinical uses of CNIR800. For

example, we can envision the use of microendoscopic systems for detection of CNIR800 signal in the lungs and intestines of humans, as well as reflective systems for detection of signal in skin.

Figure Legends

Figure 1. The structure and fluorescence emission of CNIR800. (*A*) Structure of CNIR800. IRDye 800CW is linked to a quencher (QC-1) via a lactam ring, which can be hydrolyzed by Mtb BlaC (β-lactamase). (*B*) *In vitro* fluorescence emission spectra of CNIR800 after hydrolysis with BlaC (1 µM) over time of incubation with the enzyme BlaC from 2-120 min. (C) Fluorescence over time of CNIR800 (4 µM) hydrolysis with and without BlaC treatment (1 µM) as compared to the solvent, phosphate buffered saline (PBS).

Figure 2. *In vitro* detection of mycobacteria with CNIR800 and kinetics of CNIR800 in the blood of uninfected mice. Fluorogenic substrate CNIR800 allows detection of mycobacteria by fluorescence confocal microscopy (A) and spectrophotometer (B). (A) J774A.1 murine macrophages were infected with GFP (green) expressing *M. bovis* BCG strain and co-incubated with CNIR800 substrate (red) for 30 min. Fixed cells were stained with DAPI (blue) to visualize nuclei. The scale bars are 10 µm. (*B*) Broad range of *M. bovis* BCG strain was co-incubated with CNIR800 and measured fluorescence using a spectrophotometer. Correlation of the fluorescence with the number of bacteria present in each well was determined using a Pearson's correlation test. Statistical

significance was determined using a Student's 2-tailed *t*-test with significance set at **P*<0.05 comparing to 10^0 bacteria group. Experiment was done in triplicate.

For the kinetic test, CNIR800 (20 µM) was delivered to uninfected mice by intraperitoneal injection. Blood was collected at various times post-administration of CNIR800. (*C*) Blood was incubated with 10 ng/µl of BlaC or without BlaC and fluorescent signal was measured using a whole animal imaging system. (*D*) Quantification of fluorescence from the blood incubated with or without BlaC treatment over time post-administration of CNIR800. Statistical significance was determined using a Student's 2-tailed *t*-test with significance set at **P*<0.05, ***P*<0.01 comparing with BlaC to no BlaC at the same time point.

Figure 3. Tissue distribution of CNIR800 in uninfected mice. Organs were collected from uninfected mice with CNIR800 administration (20 µM, 2.5 ul/g, I.P) over 1-24 h post-administration. (*A*) Excised organ images taken with epi-illumination. (*B*) Quantification of fluorescence in organs over time post-administration of CNIR800. (*C*) Zoomed in graph of the asterisk in (*B*). LN = lymph node.

Figure 4. Kinetics of fluorescence in mice infected with Mtb. Mice were infected with 5 × 10^6 CFU of Mtb strain Erdman I.V. and administered with CNIR800 (20 uM, 2.5 ul/g, I.P.) at 24 h post-infection. At the indicated time post-administration of CNIR800, images were taken and fluorescence was measured followed by collecting lungs, *ex vivo* lung imaging, homogenization, and plating for CFU. The CFU present in the lungs were

between 3 and 4.5 x 10^6 CFU at all time points shown. (*A*) Whole body images were taken using trans-illumination at indicated time post-administration of CNIR800. (*B*) *Ex vivo* lung images were taken using epi-illumination after whole body images.

Figure 5. Threshold determination and correlation of fluorescence with bacterial numbers in the lungs. Groups of mice were infected with different concentrations of Mtb strain CDC1551 intratracheally and at 24 h post-infection, CNIR800 (20 µM, 2.5 µl/g) was administered intraperitoneally. (*A*) Mouse whole body images taken using trans-illumination at 6 h post-administration of CNIR800. Following whole body imaging, mice were euthanized to collect the lungs. The lungs were imaged, homogenized and plated to determine CFU. (*B*) *Ex vivo* lung images taken by epi-illumination. (*C*) Correlation of fluorescence in whole body images to bacterial CFU in the lungs. (*D*) Correlation between fluorescence in excised lungs and bacterial CFU in the lungs. Correlation was determined using Pearson correlation test with significance set at *** $P \leq 0.001$.

Figure 6. Evaluation of therapeutic efficacy by REF imaging using CNIR800 in mice. Mice were infected with ~50 CFU of Mtb strain CDC1551 by a Madison chamber. Equivalent groups of four animals were either untreated or treated with different concentrations of isoniazid (INH) of 5, 1 and 0.1 mg/kg at week 2 post-infection for 4 weeks (Week 2-6, shown by red box in A, B and C) daily by intraperitoneal administration. Mice were imaged at the indicated time points post-infection with CNIR800 administration

followed by collecting the lungs, homogenization, and plating for CFU. (*A*) Whole body images taken at 6 h post-administration of CNIR800 (20 uM, 2.5 ul/g, I.P) by trans-illumination. INH was given at 5 mg/kg to the mice daily. (*B, D*) Comparison of fluorescence over time with 5 mg/kg (B), and various concentrations of INH treatment (D). (*C, E*) Comparison of bacterial loads in the lungs over time with 5 mg/kg (C), and various concentrations of INH treatment (D). Data represent the means and standard deviations for each group of animals. Statistical significance was determined using a Student's 2-tail *t*-test with significance set at $^{**}P<0.01$, $^{***}P<0.001$ as compared to treated animals at the same time point or $^{++}P<0.01$, $^{+++}P<0.001$ as compared to uninfected animals at the same time point (*B, C*) or ANOVA with significance set at $^{***}P<0.001$ (*D, E*). WK = Week; INH = isoniazid.

References

1. Dye C, Bassili A, Bierrenbach AL, et al. Measuring tuberculosis burden, trends, and the impact of control programmes. Lancet Infect Dis **2008**; 8:233-43.

2. Kong Y, Yao H, Ren H, et al. Imaging tuberculosis with endogenous beta-lactamase reporter enzyme fluorescence in live mice. Proc Natl Acad Sci U S A **2010**; 107:12239-44.

3. Kong Y, Subbian S, Cirillo SL, Cirillo JD. Application of optical imaging to study of extrapulmonary spread by tuberculosis. Tuberculosis (Edinb) **2009**; 89 Suppl 1:S15-7.

4. Kong Y, Cirillo JD. Reporter enzyme fluorescence (REF) imaging and quantification of tuberculosis in live animals. Virulence **2010**; 1:558-62.

5. Kong Y, Akin AR, Francis KP, et al. Whole‐Body Imaging of Infection Using Fluorescence. Curr Protoc Microbiol **2011**:2C. 3.1-2C. 3.21.

6. Chang M, Cirillo SL, Cirillo JD. Using luciferase to image bacterial infections in mice. J Vis Exp **2011**.

7. Chang M, Anttonen KP, Cirillo SL, Francis KP, Cirillo JD. Real-time bioluminescence imaging of mixed mycobacterial infections. PLoS One **2014**; 9:e108341.

8. Chang M, Anttonen KP, Cirillo SLG, Francis KP, Cirillo JD. Real-Time Bioluminescence Imaging of Mixed Mycobacterial Infections. PLoS ONE **2014**; 9:e108341.

9. Flores AR, Parsons LM, Pavelka MS, Jr. Genetic analysis of the beta-lactamases of Mycobacterium tuberculosis and Mycobacterium smegmatis and susceptibility to beta-lactam antibiotics. Microbiology **2005**; 151:521-32.

10. Hugonnet JE, Tremblay LW, Boshoff HI, Barry CE, 3rd, Blanchard JS. Meropenem-clavulanate is effective against extensively drug-resistant Mycobacterium tuberculosis. Science **2009**; 323:1215-8.

11. Weissleder R. A clearer vision for in vivo imaging. Nat Biotechnol **2001**; 19:316-7.

12. Xie H, Mire J, Kong Y, et al. Rapid point-of-care detection of the tuberculosis pathogen using a BlaC-specific fluorogenic probe. Nat Chem **2012**; 4:802-9.

13. Cheng Y, Xie H, Sule P, et al. Fluorogenic Probes with Substitutions at the 2 and 7 Positions of Cephalosporin are Highly BlaC‐Specific for Rapid Mycobacterium tuberculosis Detection. Angew Chem Int Ed Engl **2014**; 53:9360-4.

14. Cirillo SL, Subbian S, Chen B, Weisbrod TR, Jacobs WR, Jr., Cirillo JD. Protection of Mycobacterium tuberculosis from reactive oxygen species conferred by the mel2 locus impacts persistence and dissemination. Infect Immun **2009**; 77:2557-67.

15. Cohen MK, Bartow RA, Mintzer CL, McMurray DN. Effects of diet and genetics on Mycobacterium bovis BCG vaccine efficacy in inbred guinea pigs. Infect Immun **1987**; 55:314-9.

16. Gordon S, Keshav S, Stein M. BCG-induced granuloma formation in murine tissues. Immunobiology **1994**; 191:369-77.

17. Nerli B, Pico G. Evidence of human serum albumin beta-lactamase activity. Biochem Mol Biol Int **1994**; 32:789-95.

18. Ahmad E, Rabbani G, Zaidi N, Ahmad B, Khan RH. Pollutant-induced modulation in conformation and beta-lactamase activity of human serum albumin. PLoS One **2012**; 7:e38372.

19. Marshall MV, Draney D, Sevick-Muraca EM, Olive DM. Single-dose intravenous toxicity study of IRDye 800CW in Sprague-Dawley rats. Mol Imaging Biol **2010**; 12:583-94.

20. Padilla-Carlin DJ, McMurray DN, Hickey AJ. The Guinea Pig as a Model of Infectious Diseases. Comp Med **2008**; 58:324-40.

21. McMurray DN. Disease model: pulmonary tuberculosis. Trends Mol Med **2001**; 7:135-7.

22. McMurray DN. Guinea pig model of tuberculosis. Tuberculosis: pathogenesis, protection, and control American Society for Microbiology, Washington, DC **1994**:135-47.

23. Weissleder R, Ntziachristos V. Shedding light onto live molecular targets. Nat Med **2003**; 9:123-8.

24. Balas C. Review of biomedical optical imaging—a powerful, non-invasive, non-ionizing technology for improving in vivo diagnosis. Meas Sci Technol **2009**; 20:104020.

25. Foster AE, Kwon S, Ke S, et al. In vivo fluorescent optical imaging of cytotoxic T lymphocyte migration using IRDye800CW near-infrared dye. Appl Opt **2008**; 47:5944-52.

26. Cohen R, Stammes MA, de Roos IH, Stigter-van Walsum M, Visser GW, van Dongen GA. Inert coupling of IRDye800CW to monoclonal antibodies for clinical optical imaging of tumor targets. EJNMMI Res **2011**; 1:31.

27. Kijanka M, Warnders FJ, El Khattabi M, et al. Rapid optical imaging of human breast tumour xenografts using anti-HER2 VHHs site-directly conjugated to IRDye 800CW for image-guided surgery. Eur J Nucl Med Mol Imaging **2013**; 40:1718-29.

28. van Oosten M, Schäfer T, Gazendam JA, et al. Real-time in vivo imaging of invasive- and biomaterial-associated bacterial infections using fluorescently labelled vancomycin. Nat Commun **2013**; 4.

29. Kwon HH, Tomioka H, Saito H. Distribution and characterization of beta-lactamases of mycobacteria and related organisms. Tuber Lung Dis **1995**; 76:141-8.

30. Cheng Y, Xie H, Sule P, et al. Fluorogenic Probes with Substitutions at the 2 and 7 Positions of Cephalosporin are Highly BlaC‐Specific for Rapid Mycobacterium tuberculosis Detection. Angew Chem Int Ed Engl **2014**; 126:9514-8.

31. Zhang Y, Steingrube VA, Wallace RJ, Jr. beta-Lactamase inhibitors and the inducibility of the beta-lactamase of Mycobacterium tuberculosis. Am Rev Respir Dis **1992**; 145:657-60.

32. Fattorini L, Scardaci G, Jin SH, et al. Beta-lactamase of Mycobacterium fortuitum: kinetics of production and relationship with resistance to beta-lactam antibiotics. Antimicrob Agents Chemother **1991**; 35:1760-4.

33. McDonough JA, Hacker KE, Flores AR, Pavelka MS, Braunstein M. The twin-arginine translocation pathway of Mycobacterium smegmatis is functional and required for the export of mycobacterial β-lactamases. J Bacteriol **2005**; 187:7667-79.

34. Saint-Joanis B, Demangel C, Jackson M, et al. Inactivation of Rv2525c, a substrate of the twin arginine translocation (Tat) system of Mycobacterium tuberculosis, increases beta-lactam susceptibility and virulence. J Bacteriol **2006**; 188:6669-79.

35. Posey JE, Shinnick TM, Quinn FD. Characterization of the twin-arginine translocase secretion system of Mycobacterium smegmatis. J Bacteriol **2006**; 188:1332-40.

Footnotes

Financial support.

This work was supported by the National Heart, Lung, and Blood Institute and the National Institute of Allergy and Infectious Diseases of the National Institutes of Health grants HL115463 (YK) and AI104960 (JDC) and by grant 48523 (JDC) from the Bill & Melinda Gates Foundation.

Potential conflicts of interest.

JDC and JR own significant stock in and consults for GlobalBioDiagnostics Corp., who have licensed the REF technology. All other authors report no potential conflicts.

Correspondence.

Jeffrey D. Cirillo; Department of Microbial Pathogenesis and Immunology, Texas A&M Health Science Center, Bryan, TX 77807; Tel. 979-436-0343; Fax 979-436-0360; JDCirillo@medicine.tamhsc.edu

Figure 1.

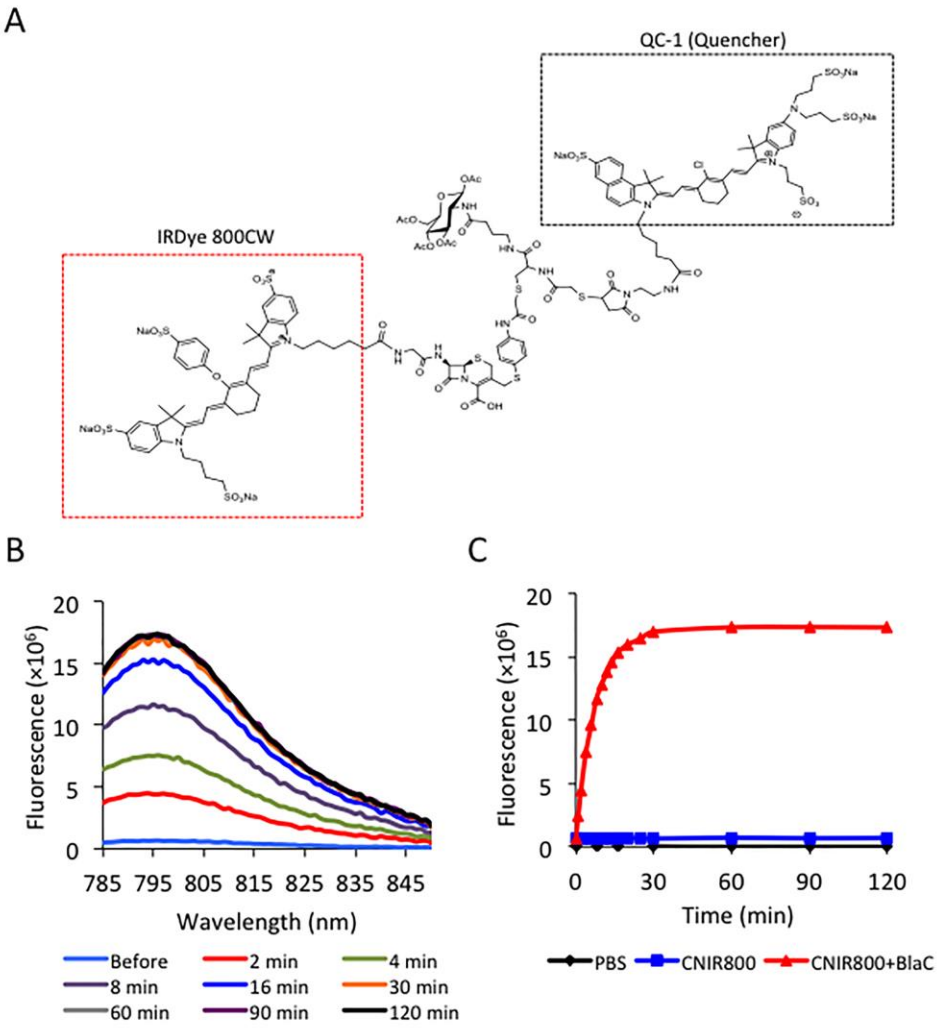
A
QC-1 (Quencher)
IRDye 800CW
B
Fluorescence (×10⁶)
20
15
10
5
0
785 795 805 815 825 835 845
Wavelength (nm)
Before
2 min
4 min
8 min
16 min
30 min
60 min
90 min
120 min
C
Fluorescence (×10⁶)
20
15
10
5
0
0 30 60 90 120
Time (min)
PBS
CNIR800
CNIR800+BlaC

Figure 2.

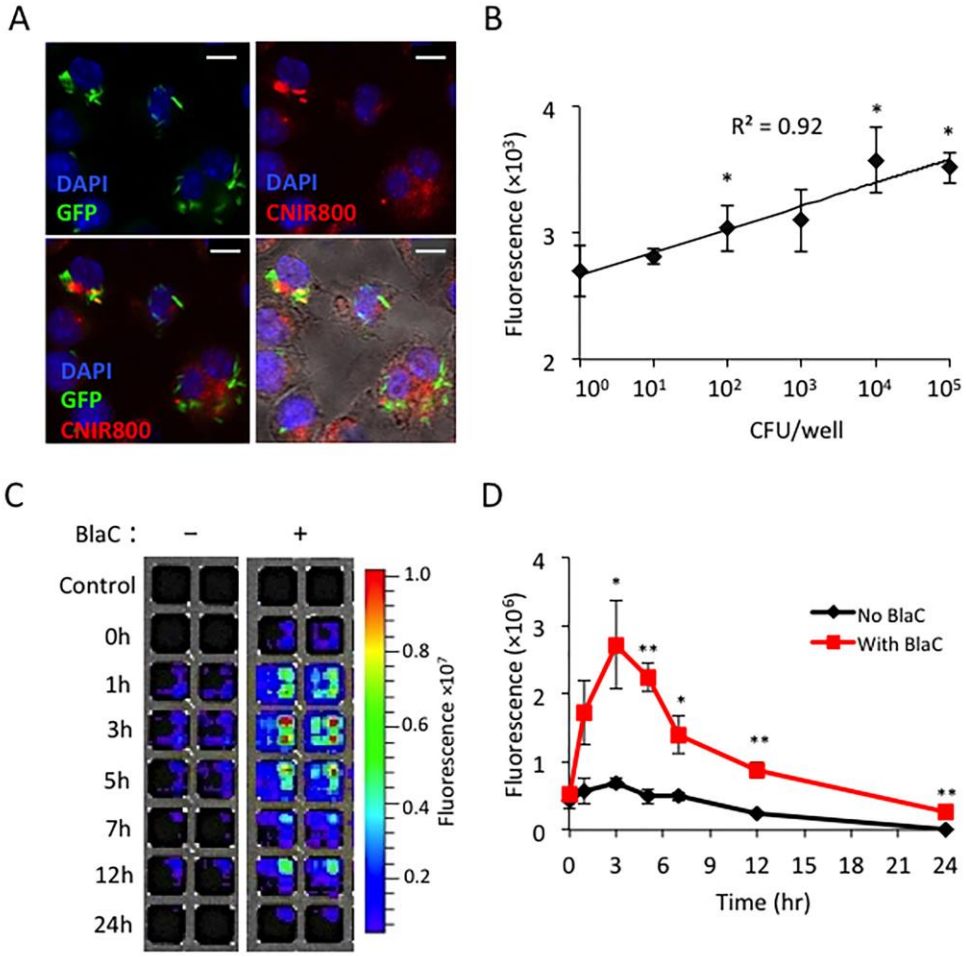
A
DAPI
GFP
DAPI
CNIR800
DAPI
GFP
CNIR800
B
R² = 0.92
Fluorescence (×10³)
CFU/well
C
BlaC :
Control
0h
1h
3h
5h
7h
12h
24h
Fluorescence ×10⁷
D
No BlaC
With BlaC
Fluorescence (×10⁶)
Time (hr)

Figure 3.

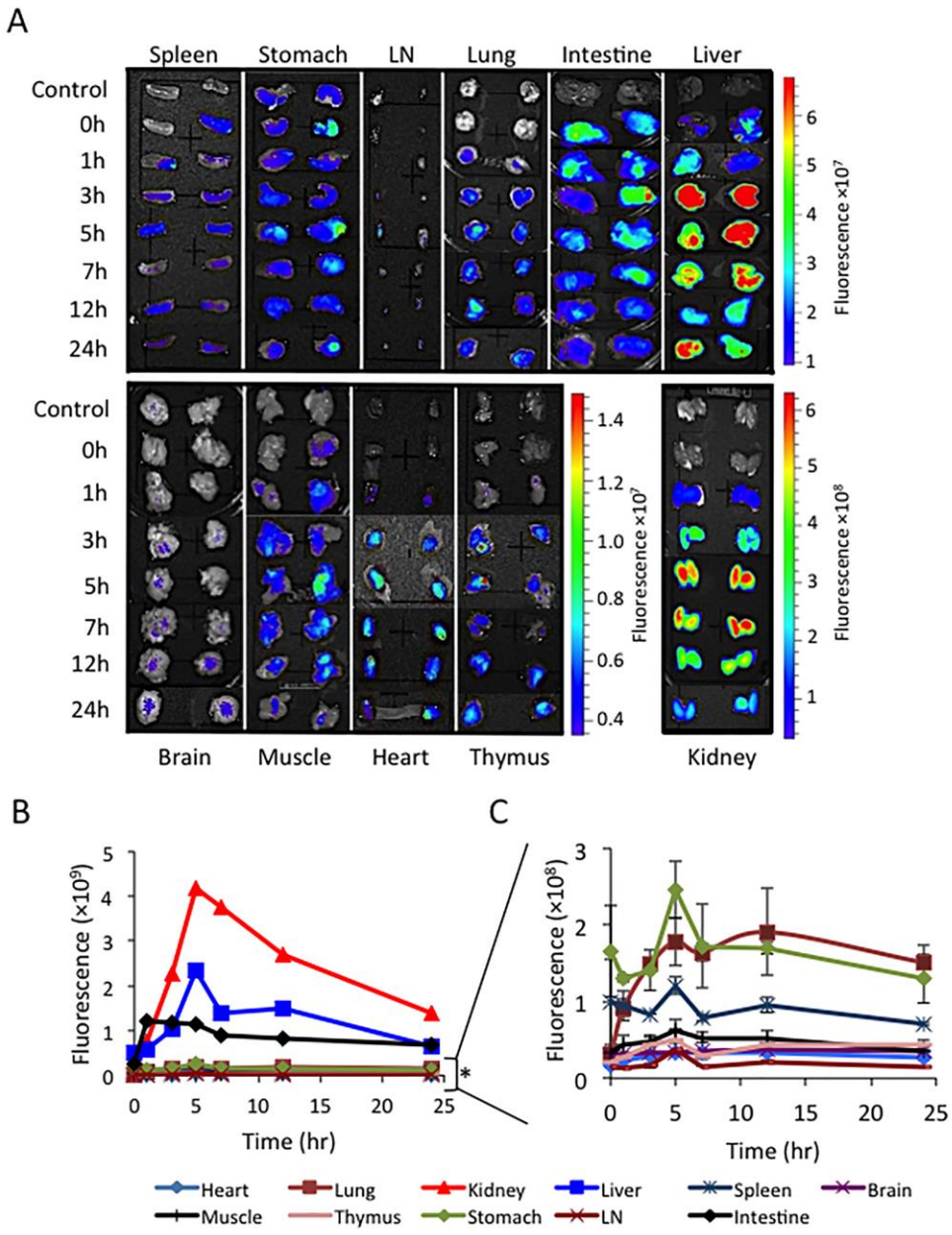
A
Spleen
Stomach
LN
Lung
Intestine
Liver
Control
0h
1h
3h
5h
7h
12h
24h
Fluorescence ×10⁷
Fluorescence ×10⁸
Brain
Muscle
Heart
Thymus
Kidney
B
C
Fluorescence (×10⁹)
Fluorescence (×10⁸)
Time (hr)
Heart
Lung
Kidney
Liver
Spleen
Brain
Muscle
Thymus
Stomach
LN
Intestine

Figure 4.

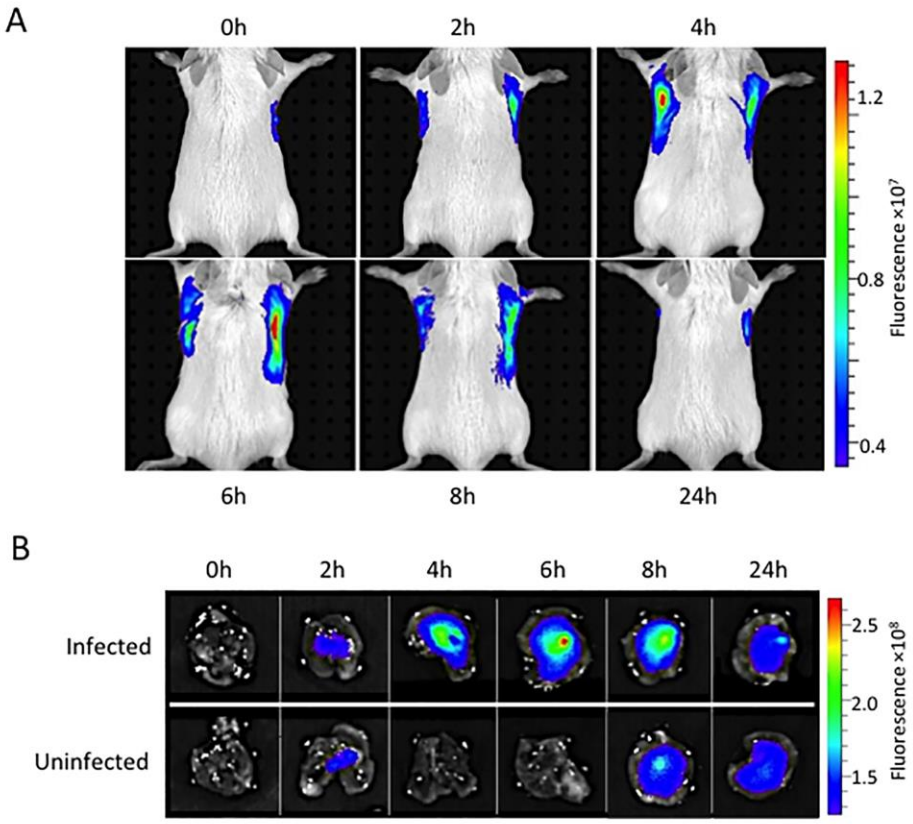
A
0h
2h
4h
6h
8h
24h
1.2
0.8
0.4
Fluorescence ×10⁷
B
0h
2h
4h
6h
8h
24h
Infected
Uninfected
2.5
2.0
1.5
Fluorescence ×10⁸

Figure 5.

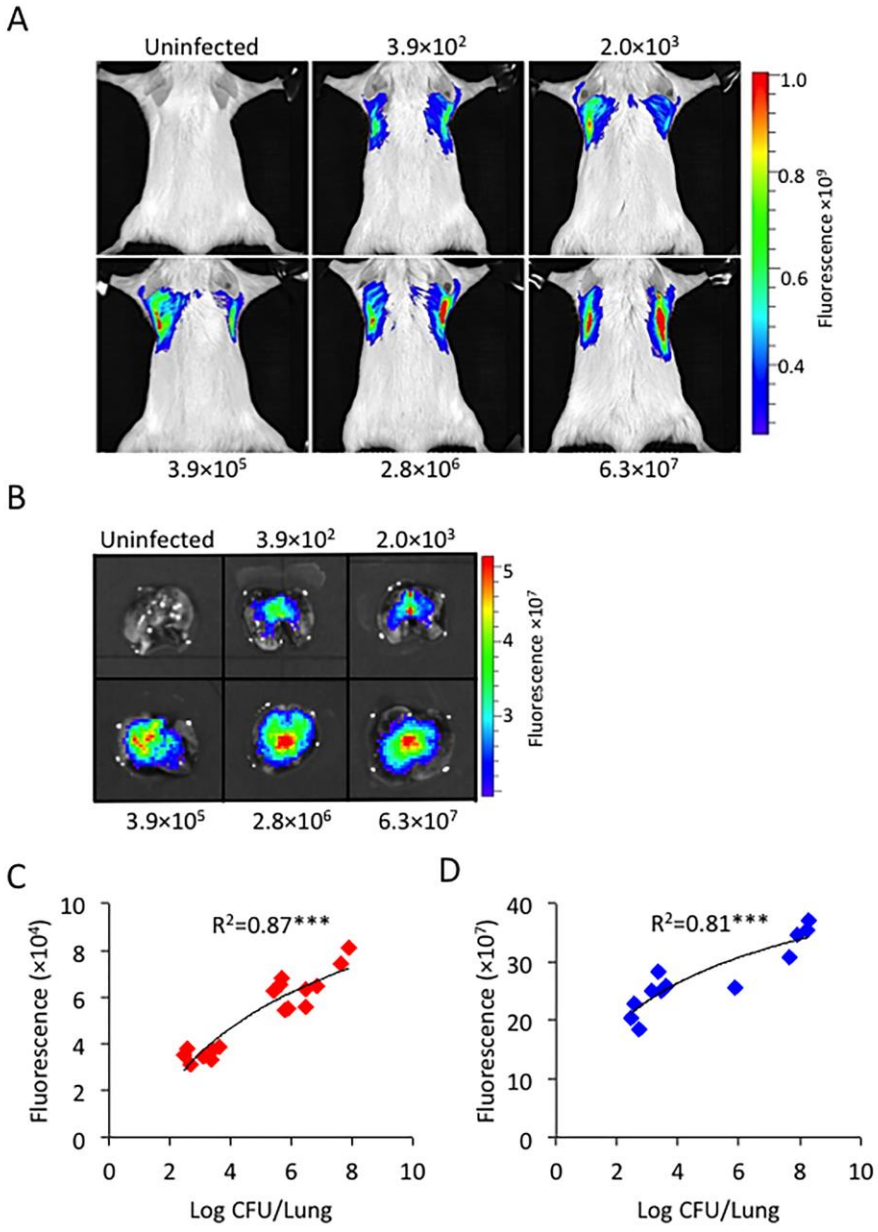
A
Uninfected
3.9×10²
2.0×10³
3.9×10⁵
2.8×10⁶
6.3×10⁷
1.0
0.8
0.6
0.4
Fluorescence ×10⁹
B
Uninfected
3.9×10²
2.0×10³
3.9×10⁵
2.8×10⁶
6.3×10⁷
5
4
3
Fluorescence ×10⁷
C
R²=0.87***
Fluorescence (×10⁴)
Log CFU/Lung
D
R²=0.81***
Fluorescence (×10⁷)
Log CFU/Lung

Figure 6.

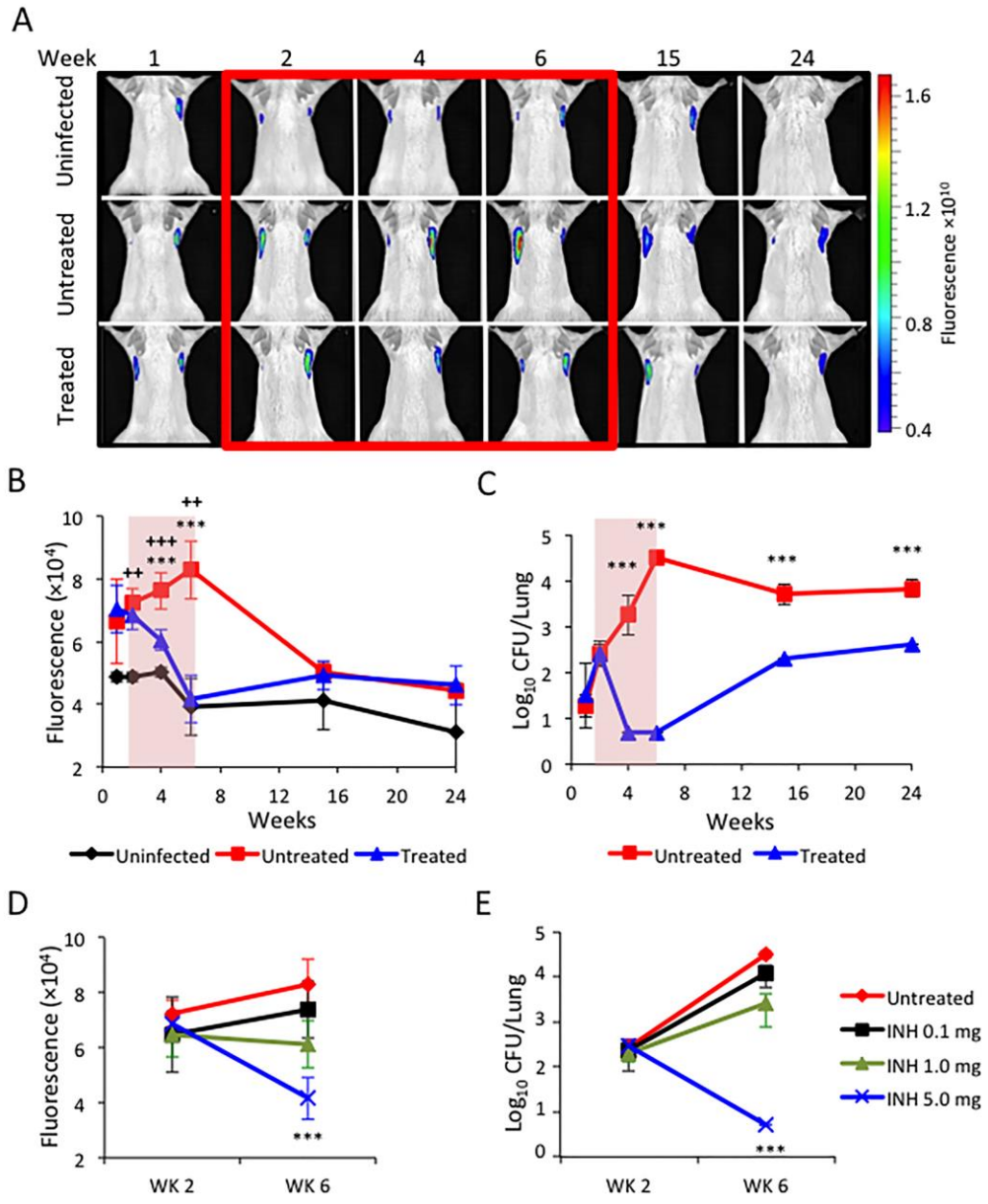
A
Week
1
2
4
6
15
24
Uninfected
Untreated
Treated
1.6
1.2
0.8
0.4
Fluorescence ×10¹⁰
B
Fluorescence (×10⁴)
Weeks
Uninfected
Untreated
Treated
C
Log10 CFU/Lung
Weeks
Untreated
Treated
D
Fluorescence (×10⁴)
WK 2
WK 6
E
Log10 CFU/Lung
WK 2
WK 6
Untreated
INH 0.1 mg
INH 1.0 mg
INH 5.0 mg